# CHARLES UNIVERSITY IN PRAGUE

Faculty of Science

**Department of Physical and Macromolecular Chemistry**


Program: Chemistry

Field of study: Physical chemistry



**Bc. Juraj Škvarla**


Nanočástice na bázi komplexů blokových kopolymerů s fluorovanými surfaktanty

Nanoparticles based on block copolymer complexes with fluorosurfactants

**Diploma thesis**

Advisor: RNDr. Miroslav Štěpánek, Ph.D.

Prague, 2012

**Annotation:**

This thesis deals with (i) complex nanoaggregates of cationic perfluorinated surfactant N-(1,1,2,2-tetrahydroperfluorodecyl)pyridinium chloride and of double hydrophilic block polyanions poly(ethylene oxide)-b-poly(methacrylate) and poly(ethylene oxide)-b-poly((2-sulfamate-3-carboxylate)isoprene), and with (ii) mixed micelles of amphiphilic copolymer poly(ethylene oxide)-b-poly(e-caprolactone) and nonionic perfluorinated fluorosurfactant Zonyl FSN-100. The study was aimed at the characterization of the association behavior of the block copolymer–fluorosurfactant systems in aqueous solutions depending on the amount of the added surfactant, pH of the solvent and the structure of the copolymers.

**Key words:**

polyion complex micelles, double hydrophilic block copolymers, perfluorinated surfactants, nuclear magnetic resonance

**Anotace:**

Práce se zabývá (i) komplexními nanoagregáty kationtového perfluorovaného surfaktantu N-(1,1,2,2-tetrahydroperfluorodecyl)pyridinium chloridu s dvojitě hydrofilními blokovými polyanionty polyoxyethylen-b-polymethakrylátem a poly(oxyethylen)-b-poly(2-sulfamát-3-karboxylát)isoprenem, a (ii) směsnými micelami vzniklými z poly(oxyethylen)-b-poly(e-kaprolakton)u a neiontového fluorovaného surfaktantu Zonyl FSN-100. Toto studium bylo zaměřeno na charakterizaci asociačního chování systémů blokový kopolymer–perflurovaný surfaktant ve vodných roztocích v závislosti na množství přidaného surfaktantu, pH a struktuře kopolymerů.

**Klíčova slova:**

polyiontové micelární komplexy, dvojité hydrofilní kopolymery, fluorované surfaktanty, nukleární magnetická rezonance

# Statement

This diploma thesis has been elaborated at the Department of Physical and Macromolecular Chemistry, Faculty of Science, Charles University of Prague in years 2010 – 2012. I have been led by RNDr. Miroslav Štěpánek, PhD. I declare that I have elaborated this work on my own and all the literature used is properly cited. Neither this work, nor its parts have been used for the acquirement of an academic degree.

# Prohlášení:

Prohlašuji, že jsem závěrečnou práci zpracoval samostatně a že jsem uvedl všechny použité informační zdroje a literaturu. Tato práce ani její podstatná část nebyla předložena k získání jiného nebo stejného akademického titulu.

In Prague 27.4.2012 …….

Signature

First I would like to thank Mr. RNDr. Miroslav Štěpánek, PhD. for supervising me, for his patience and interest in solving problems that arose during elaboration of this work. I would also like to thank to Dr. M. Šlouf, Institute of Macromolecular Chemistry, Academy of Sciences of the Czech Republic and to Ing. L. Kováčik, 1st Faculty of Medicine, Charles University for TEM and *cryo*-TEM measurements. Then I would like to thank to Prof. RNDr. Karel Procházka, DrSc. Big thank to my family, especially to my parents, my brothers and my girlfriend for their understanding, encouragement and trust.

# Abbreviations

| | |
|---|---|
| ABC | Amphiphilic block copolymers |
| *cryo*-TEM | Cryogenic temperature transmission electron microscopy |
| DHBC | Double hydrophilic block copolymer |
| DLS | Dynamic light scattering |
| QNPHOS | poly[3,5-bis(trimethylammoniummethyl)4-hydroxystyrene iodide] |
| GMA | Globular micelle aggregates |
| HFDPCl | 1,1,2,2-tetrahydro-perfluorodecyl pyridinium chloride |
| MM | Mixed micelles |
| MRI | Magnetic resonance imaging |
| MRS | Magnetic resonance spectroscopy |
| NMR | Nuclear magnetic resonance |
| PCL | Polycaprolactone |
| PEO | poly(ethylene oxide) |
| PIC | Polyion complex |
| PSCI | poly((sulfamate-carboxylate)isoprene) |
| SLS | Static light scattering |
| TEM | Transmission electron microscopy |
| Zonyl | Zonyl FSN-100 |

In the text, block copolymers are mostly referred by abbreviations of their segments, such as PEO-PMAA instead of PEO-*b*-PMAA for poly(ethylene oxide)-*b*-poly(methacrylate).

# Contents

**1. Introduction** ..... **7**
1.1 Present research and use of $^{19}F$ as a NMR probe ..... 7
1.2 Double hydrophilic block copolymers ..... 9
1.3 Amphiphilic block copolymers ..... 11
1.4 Perfluorinated surfactants ..... 11
1.5 Theory of characterization methods ..... 12
1.5.1 Static light scattering ..... 12
1.5.2 Dynamic light scattering ..... 14
1.5.3 Transmission electron microscopy ..... 16
1.5.4 Cryogenic transmission electron microscopy ..... 17
**2. Experimental section** ..... **18**
2.1 Materials ..... 18
2.1.1 Copolymers ..... 18
2.1.2 Surfactants ..... 19
2.2 Preparation of nanoparticles ..... 20
2.3 Methods ..... 22
2.3.1 Light scattering measurements ..... 22
2.3.2 Transmission electron microscopy measurements ..... 23
2.3.3 Cryogenic transmission electron microscopy ..... 23
2.3.4 Nuclear magnetic resonance ..... 23
**3. Results and discussion** ..... **24**
3.1 $PSCI_{62}$-$PEO_{259}$ ..... 24
3.1.1 Particles prepared in 0.1 M HCl ..... 24
3.1.2 Particles prepared in 0.05 M sodium tetraborate buffer ..... 26
3.2 $PSCI_{70}$-$PEO_{1289}$ ..... 31
3.2.1 Particles prepared in 0.1 M HCl ..... 31
3.2.2 Particles prepared in 0.05 M Sodium tetraborate buffer ..... 33
3.3 PMAA-PEO ..... 35
3.4 Amphiphilic PCL-PEO/Zonyl aggregates ..... 37
3.5 NMR measurements ..... 38
**4. Conclusion** ..... **40**
**5. References** ..... **42**

# 1. Introduction

This work focuses on developing and describing new self-assembled nanosized complexes based on double hydrophilic block copolymers and low molecular weight fluorinated surfactants in aqueous media as well as nanoparticles formed from amphiphilic block copolymers and nonionic fluorinated surfactants. These nanoparticles could represent a new alternative to fluorinated molecules that are already being developed primary as a medical diagnostic tool, mainly for the magnetic resonance imaging and spectroscopy. The preparation of such self-assembled nanoparticles formed via electrostatic and hydrophobic interactions between block copolymers and fluorinated surfactants will be followed by physicochemical characterization techniques such as light scattering, transmission electron spectroscopy, cryogenic transmission electron microscopy and NMR spectroscopy.

## *1.1 Present research and use of $^{19}F$ as a NMR probe*

Potential applications of $^{19}F$ imaging and spectroscopy for obtaining functional information in living organisms were suggested first in the 1970s, which was around the time of the first $^{1}H$ MRI application in the human medicine [1]. $^{19}F$ has the nuclear spin of ½ and the NMR frequency at 1T of 40.077 MHz (in comparison with $^{1}H$ with 42.576 MHz at 1T). The NMR sensitivity of $^{19}F$ is 0.83 relative to $^{1}H$. The high gyromagnetic ratio of $\gamma = 25.177.10^{7}$ $T^{-1}s^{-1}$ is only 6% lower than that of $^{1}H$ protons allowing for making measurements quickly, compared with proton magnetic resonance measurements and the use of existing NMR instrumentation with a minimum of component adjustments. The $^{19}F$ chemical shift is extremely sensitive to the molecular environment of the nucleus, mainly because of seven outer-shell electrons. In comparison with the $^{1}H$ chemical shift, which varies in the range of about 10 ppm, the fluorine chemical shift manifests itself in the range of ~300 ppm [2]. Although it is not one of basic NMR active nuclei used in science and medicine, fluorine is still commonly used in nuclear magnetic resonance, especially in the study of protein structures and conformational changes [3]. Fluorine occurs in the human

body, but it is present mostly in the form of solid fluorides in bones and teeth. Endogenous fluorine has a very short $T_2$ relaxation time and the resulting signal is below the limits of NMR detection in most biological systems of interest. Thus, exogenously administered fluorine containing compounds or particles is observed without interference from the background signal [4,5]. There are already many different molecular agents designed for this purpose. We can divide such agents into three groups: (a) "active agents", designed to interact with the environment in which fluorine atoms respond to specific parameters, such as ion concentration, enzyme activity or $pO_2$ (mainly through magnetic resonance spectroscopy), (b) "passive agents", which occupy a space to reveal tissue properties by the NMR signal, while remaining inert (through magnetic resonance imaging) and (c) fluorinated pharmaceuticals suitable for NMR investigations.

Perfluorocarbon nanoemulsions are one of the most widely studied (PFCs, molecules similar to common organic compounds, e.g. alkanes, except all of hydrogen atoms are replaced by fluorine) for this purpose but there are also other molecular systems under investigation such as perfluorinated amphiphilic copolymers [6-9]. All of those agents are based on incorporating highly fluorinated compounds into the body. The main problem related to the incorporation of perfluorinated molecules to the human body is that they are both hydrophobic and lipophobic. That's why PFCs are typically emulsified in the nanoparticle form for relevant biological applications.

Another way to bypass this problem could be a functionalization of these perfluorinated molecules. Their conversion into the ionic form would not only increase their hydrophilicity, but more importantly open new ways how to incorporate these highly fluorinated molecules into the body [10]. One way to achieve this could be complexation with double hydrophilic block copolymers (DHBC) to form polyion complex (PIC) nanoparticles. In the case of nonionic forms, amphiphilic perfluorinated surfactants could form mixed micelles (MM) with amphibhilic block copolymer (ABC) micelles. These particles (PIC as well as MM) would be water soluble and thus they could be easily incorporated into living organisms.

Potential applications are manifold. For example, passive agents could be used for cell tracking [11], as contrast agents [12] or as imaging agents for drug delivery systems [13].

## *1.2 Double hydrophilic block copolymers*

DHBCs consist of two hydrophilic blocks of different chemical nature. These polymers are typically rather small, having block with molar mass between $10^3 – 10^4$ g/mol with both chains being water soluble.

Here we will focus on DHBCs where one of the blocks is polyelectrolyte. Polyelectrolytes after chain neutralization (in our case after addition of a surfactant) precipitate, whereas DHBCs with polyelectrolyte chains do not. It is due to the nonelectrolyte hydrophilic block. Instead, these copolymers behave similarly to amphiphilic block copolymers. Their amphiphilic nature manifests itself in the surface activity or micelle formation, appearing under the influence of given external stimuli. Induction of water insolubility of one of the blocks can be achieved by a variation of temperature, pH [14] or ionic strength. It can be further induced by a complex formation of one of their blocks by electrostatic interaction with oppositely charged polyelectrolyte or surfactant molecules or by the complexation with metals to form polyion complex micelle (PIC) aggregates [15-17]. Such block ionomer complexes can be depicted as amphiphilic supramolecular block copolymers, in which the nonionic block functions as the hydrophilic part, while the electrostatic complex of the ionic block and aggregated surfactant counterions serves as the hydrophobic part. PIC aggregates are potential alternatives to classical amphiphilic block copolymers (ABC) as drug carrying agents. Their biggest advantage is that in comparison with ABCs they can solubilize ionic drugs or other ionic substances (e.g. DNA, polyions, enzymes, RNA, perfluorinated surfactants) and keep them within the hydrophobic core. Another advantage of this approach is that such assemblies are formed in water and no organic solvent is required for their preparation [18-20]. Parameters influencing biodistribution in body or clearance body time are mainly the size, shape, surface charge and the affinity to proteins [21]. The most important properties related to magnetic resonance are the signal-to-noise ratio and $T_1$, $T_2$ relaxation times, which in

turn depends on the nature of the nanoassemblies. The complex solubility and macroscopic aggregate characteristics depend not only on the length of the nonionic hydrophilic block but also on the polyion block length and the structure of the surfactant molecule. By varying molecular characteristics of the copolymer and the surfactant, their mixing ratio, total concentration and preparation method, it could be possible to prepare tailor-made nanoparticles for particular application [22-26].

As the PIC nanoaggregate formation is driven by the insolubilization of the polyelectrolyte chain, the amount of added surfactant and its total concentration are very important parameters. Here we define the apparent degree of neutralization as follows:

$$DN(\%) = \frac{z_{\text{surf}}}{z_{\text{pol}}} \times 100 \qquad (1)$$

where the $z_{\text{surf}}$ is the amount of charged functional groups from the surfactant and $z_{\text{pol}}$ is the total charge number of the polyelectrolyte.

It was also found that the properties of PIC aggregates strongly depend on the hydrophobicity of the surfactant chains [27, 28]. Hence, it is suitable to expect a different behavior of PIC aggregates formed by the interaction of perfluorinated surfactants with DHBCs and those formed by the interaction of their corresponding hydrogenated analogs with DHBCs.

Poly(ethylene oxide) (PEO or PEG) is one of the most popular hydrophilic polymers used for biomedical applications. It is considered fully biocompatible. Particles coated by this polymer are tolerated by living organisms and exhibit very low adsorption affinity to proteins. Depending on molecular weight, it is used in many areas such as cosmetics, food industry, pharmaceutics, biomedicine, etc. Because of its low adsorption to proteins, it is possible to prepare nanoassemblies with „stealth“ effect for a prolonged blood circulation. That is why in all of here studied DHBC copolymers PEO chains form the hydrophilic part [35,36].

## *1.3 Amphiphilic block copolymers*

Amphiphilic block copolymers consist of a hydrophilic and hydrophobic block. Therefore, they may be considered polymeric analogues to low molecular surfactants. Indeed they behave similarly to low molecular surfactants, but they have a much lower critical micelle concentration (CMC) and a slower exchange kinetics. ABCs undergo self-assembly in aqueous solution in order to minimalize entropically unfavorable hydrophobic interactions. In comparison with DHBCs, they are not directly soluble in water. To prepare self-assemblies of such polymers we usually dissolve them in a common solvent first and then gradually replace the solvent, for example by dialysis, or by the evaporation technique. Self-assembly and resulting properties (association number, size, etc.) of the classical amphiphilic block copolymer micelles (in our case PCL-PEO) is strongly influenced by the preparation protocol (the choice of the organic solvent and the method of the copolymer transfer from the mild selective solvent into the aqueous solution). Thus, we have chosen the already proven method (according to our previous results) described in the section 2.2.

ABCs are considered potentially suitable for various biological applications such as the drug delivery but could be used to prepare fluorine rich water soluble nanoparticles of amphiphilic block copolymer/perfluorinated surfactant mixed micelles. The interactions that are driving mixing of such micelles would have in this case mainly the hydrophobic character [29-32].

## *1.4 Perfluorinated surfactants*

There are three basic types of surfactants: neutral, cationic and anionic. Cationic surfactants are fewer in number and variety compared with anionic ones, primarily due to synthetic difficulties. A typical cationic surfactant is long alkyl ammonium or pyridinium salt. Fluorine as the most electronegative element reflects the very tight binding of its valence electrons, which results both in a low atomic polarizability and relatively small size ~1,47Å. Because of the electronegativity difference between

carbon and fluorine, C-F bonds are highly polar and that contributes to their strength. It is known that fluorine makes amphiphiles more surface active and more hydrophobic with much lower CMC in comparison with hydrogenated ones [33]. The fluorocarbon chain is stiffer than the hydrocarbon one because of the bulky fluorine atoms. Hence, self-assemblies of fluorinated amphiphiles have tendency to form a structure with a less surface curvature. The low polarizability of the fluorine atoms translates into low surface energies and thus weak cohesive forces between fluorocarbon molecules, as the interaction energy arising from the London forces varies as a square of the polarizability [34]. Those weak intermolecular forces between fluorocarbon chains explain the solubility of respiratory gases and their low boiling points. Therefore, one can expect a different behavior for PIC aggregates containing perfluorinated surfactants instead of hydrogenated ones.

## *1.5 Theory of characterization methods*

### 1.5.1 Static light scattering

Static light scattering (SLS) is a technique that measures the time-averaged intensity of scattered light as a function of the scattering angle and the sample concentration to obtain the weight average molar weight $M_w$ of small particles like macromolecules, micelles or nanoaggregates. The intensity of the radiated light depends on the magnitude of the dipole induced in the macromolecule. The more polarizable the macromolecule is, the larger the induced dipole, and hence, the greater the intensity of the scattered light. The scattering intensity that a particle produces is also proportional to the product of the weight-average molecular weight and the mass concentration of the macromolecule. Twice as many molecules scatter twice as much light and by doubling the molecular mass, even while keeping the mass concentration the same, the intensity of the scattered light doubles again. Light scattering thus represents a powerful technique for monitoring the presence and formation of aggregates.

For small particles, (macromolecules much smaller than the wavelength of the incident light can be treated as if they were essentially point scatterers) which show isotropic scattering (the scattered light in the plane perpendicular to the polarization of

the incident light is independent of scattering angle), SLS can be used to make accurate molecular weight measurements at a single angle. For larger particles, each macromolecule is assumed to be made up of very small elements, each of which scatters independently of any other. This case is generally described by the so-called Rayleigh-Debye-Gans theory. Hence, SLS may need to be done over a range of concentrations and a range of angles for accurate molecular weight determination. The angular dependence of the scattering intensity provides information on the gyration radius of the particle.

It is possible to condense the results of the Rayleigh-Debye-Gans theory of light scattering into a simple equation:

$$\frac{Kc}{R(q,c)} = \frac{1}{M_w}\left(1 + \frac{1}{3}R_g^2 q^2\right) + 2A_2 c \qquad (2)$$

where $A_2$ is second viral coefficient of the scattering particle in the viral expansion of the osmotic pressure, $R_g$ is the gyration radius of the particle, $M_w$ is its weight-average molar mass, $K$ is the constant $4\pi^2 n_0^2 (dn/dc)^2/(\lambda^4 N_A)$, where $(dn/dc)$ is the refractive index increment of the scatterer with respect to the solvent and $N_A$ is the Avogadro constant, $R(q,c)$ is the excess Rayleigh ratio of the solution as a function of the concentration and the magnitude of the scattering vector,

$$q = \left(\frac{4\pi n_0}{\lambda}\right)\sin\left(\frac{\theta}{2}\right) \qquad (3)$$

where $\theta$ is a scattering angle, $n_0$ is the refractive index of the solvent and $\lambda$ is the wavelength of the incident light. Equation 2 is used for rigorous fitting the light scattering data to retrieve the molar mass, $R_g$, and the second virial coefficient for the macromolecules in solution.

### 1.5.2 Dynamic light scattering

In dynamic light scattering (DLS or QELS) measurement time-dependent fluctuations in the scattered light are measured by fast photon counter. These fluctuations exist due to the fact that the small molecules in solutions are undergoing Brownian motion and so the distance between the scatterers in the solution is constantly changing with time. The fluctuations are directly related to the rate of diffusion of the particles through the solvent. Therefore, the fluctuations can be analyzed to determine a hydrodynamic radius for the sample from their diffusion coefficient *D* by the Stokes-Einstein equation,

$$R_H = \frac{k_B T}{6\pi\eta_0 D} \tag{4}$$

where $k_B$ is Boltzman constant, *T* is the temperature, and $\eta_0$ is the viscosity of the solvent. The fluctuations are quantified via the intensity autocorrelation correlation function given by,

$$g^{(2)}(\tau) = \frac{\langle I(t) I(t+\tau) \rangle}{\langle I(t)^2 \rangle} \tag{5}$$

where $I(t)$ is the intensity of the scattered light at time *t*, and the brackets indicate averaging over all *t*. The correlation function depends on the delay $\tau$. At short time delays, the correlation is high because the particles do not have a chance to move to a great extent from the initial state that they were in. The two signals are thus essentially unchanged when compared after only a very short time interval. As the time delays become longer, the correlation decays exponentially, meaning that, after a long time period has elapsed, there is no correlation between the scattered intensity of the initial and final states. If the sample is monodisperse then the decay is simply single exponential.

Once the autocorrelation data have been generated, different mathematical approaches can be employed to determine the diffusion coefficient of the scatterers. The simplest

approach is to treat the electric field autocorrelation function as a single exponential decay. This is appropriate for a monodisperse population,

$$g^{(1)}(q,\tau) = e^{-\Gamma\tau} \tag{6}$$

where Γ is the decay rate. The Siegert equation relates the first-order autocorrelation function $g^{(1)}(q,\tau)$ with the second-order autocorrelation function $g^{(2)}(q,\tau)$ as follows:

$$g^{(2)}(q,\tau) = 1 + \beta \cdot \left[g^{(1)}(q,\tau)\right]^2 \tag{7}$$

where $\beta$ is a correction factor that depends on the geometry and alignment of the laser beam in the light scattering setup. The translational diffusion coefficient $D$ may be derived at a single angle or at a range of angles depending on the magnitude of the scattering vector,

$$\Gamma = q^2 D \tag{8}$$

where $q$ is given by equation 3. Depending on the anisotropy and polydispersity of the system, a resulting plot of $\Gamma/q^2$ vs. $q^2$ may or may not show an angular dependence. Small spherical particles will show no angular dependence.

In most cases, samples are polydisperse. Thus, the autocorrelation function is a sum of the exponential decays corresponding to each of the species in the population. The methods have been developed to extract as much useful information as possible from an autocorrelation function. There are two most popular methods. The cumulant method is one of the most popular but is valid only for small τ and sufficiently narrow $G(\Gamma)$. CONTIN is an alternative method for analyzing autocorrelation functions based on the inverse Laplace transform. It is ideal for polydisperse and multimodal systems which cannot be resolved with the cumulant method.

### 1.5.3 Transmission electron microscopy

The transmission electron microscope (TEM) operates on the same basic principles as the light microscope does, but it uses electrons instead of light. When electrons are accelerated up to high energy levels (few hundreds keV) and focused on a material, they can scatter or backscatter elastically or non-elastically, or exhibit many interactions producing different signals such as X-rays, Auger electrons or light. Some of them are used in electron microscopy. In TEM, the incoming electron beam interacts with the sample as it passes through the entire thickness of the sample. An image is formed from the interaction of these electrons transmitted through the specimen. The image is magnified and focused onto an imaging device, such as a fluorescent screen, on a layer of photographic film, or to be detected by a sensor such as a CCD camera.

What you can see with a light microscope is limited by the wavelength of light. Because, TEM uses electrons as "light source" and their much lower wavelength (the de Broglie wavelength) makes it possible to get a resolution a thousand times better than with a light microscope. The de Broglie equation shows that the wavelength of electrons is related to their energy, *E*, and, if we ignore relativistic effects, we can show approximately,

$$\lambda = \frac{h}{\sqrt{2m_0 eU\left(1+\frac{eU}{2m_0 c^2}\right)}} \tag{9}$$

where $h$ is Planck´s constant, $m_0$ is particle´s rest mass, $U$ is electrostatic potential drop, $c$ is the speed of light and $e$ is elementary charge of electrons. That is, if we speed up electrons by increasing $U$, we lower $\lambda$ and thus improve theoretical resolution. To increase the mean free path of the electron gas interaction, a standard TEM is evacuated to low pressures, typically on the order of $10^{-4}$ Pa.

In TEM, there are a few different principles of how to obtain contrast. Some methods use “diffraction contrast” or “phase contrast”. In the diffraction contrast method, the

image is sensitive to the differences in specimen thickness, distortion of crystal lattices due to defects, strain and bending. Diffraction contrast is a dominant mechanism for imaging dislocations and defects in the specimen. However, the resolution of this imaging technique is limited to 1-3 nm. Diffraction contrast mainly reflects the long-range strain field in the specimen and it is unable, however, to provide high-resolution information about the atom distribution in the specimen. By modifying the phase of the incident electron wave we can obtain so called phase contrast. Phase-contrast images are formed by removing the objective aperture entirely or by using a very large objective aperture, contrary to diffraction contrast method. This ensures that not only the transmitted beam, but also the diffracted ones are allowed to contribute to the image. Phase-contrast imaging is the highest resolution imaging technique ever developed.

### 1.5.4 Cryogenic transmission electron microscopy

Cryogenic transmission electron microscopy (cryo-TEM) works similar to standard TEM, but operates at very low temperatures. *cryo*-TEM is now accepted as the most useful tool for direct imaging self-aggregation in liquid systems. This is mainly because particles are being observed while in hydrated state, in contrast to TEM, where the specimen is unavoidably dehydrated. Modern digital imaging cryo-TEM has expanded the applicability of the technique, and made it easier to record high-resolution images of electron-beam radiation-sensitive systems.

# 2. Experimental section

## *2.1 Materials*

### 2.1.1 Copolymers

In this work we will study three different anionic DHBCs and one amphiphilic block copolymer. Structural characteristics are listed in Table 1. For structural formulae see Figure 1.

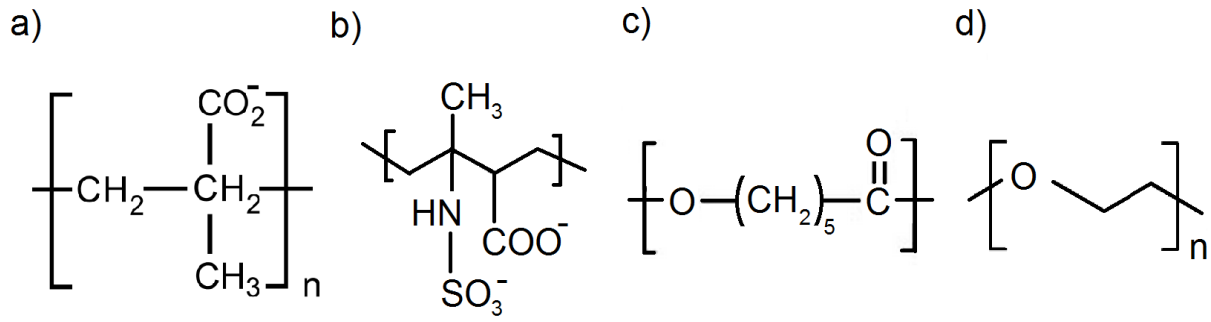


**Figure 1.** *Structural formulae of (a) anionic block of PMAA-PEO copolymer, (b) anionic block of PSCI-PEO copolymer, (c) hydrophobic block of PCL-PEO amphiphilic copolymer and (d) hydrophilic polyethylene oxide (PEO block)*

The chemical similarity between the functional groups in the sulfamate-carboxylate PI block of PSCI, and those present in heparin (a highly-sulfated glycosaminoglycan) suggests potential biotechnological uses. Both PSCI-PEO copolymers were prepared by selective postpolymerization reaction of the polyisoprene-*b*-poly(ethylene oxide) precursor with N-chlorosulfonyl isocyanate. The precursors were synthesized by high vacuum anionic polymerization technique by the group of Dr. Stergios Pispas at the Theoretical and Physical Chemistry Institute, National Hellenic Research Foundation, Athens, Greece.[37]

PCL: At physiological conditions, PCL is degradable by hydrolysis of its ester, is considered biodegradable and has therefore received a great deal of attention for potential use in biomedical applications. PCL-PEO was purchased from Aldrich.

PMAA-PEO was purchased from Polymer source Inc. Dorval, Canada.

**Table 1.** *Anionic double hydrophilic block copolymers and their structural characteristics*

| copolymer | $M_w$ [kg/mol] | $M_w$ PSC [kg/mol] | $M_w$ PEO [kg/mol] | $M_w$ PI [3] [kg/mol] | PEO units | PSC units | PI units |
|---|---|---|---|---|---|---|---|
| PSCI-PEO[1] | 27,5 | 14,3 | 11,4 | 1,8 | 259 | 62 | 26 |
| PSCI-PEO[2] | 74,3 | 16,1 | 56,7 | 1,5 | 1289 | 70 | 22 |
| PMAA-PEO | 71,7 | 41,0 | 30,7 | - | 698 | 477 | - |

*Amphiphilic block copolymers*

| copolymer | $M_w$ [kg/mol] | $M_w$ PCL[kg/mol] | $M_w$ PEO[kg/mol] | PEO units | PCL units |
|---|---|---|---|---|---|
| PCL-PEO | 37,0 | 32,0 | 5,0 | 114 | 281 |

[1], [2] *each copolymer will be further distinguished by the polymerization degree of its both chains indicated as an index, e.g.* $PSCI_{62}$-$PEO_{259}$. [3]*Note that both of PSCI-PEO copolymers, due to preparation technique contained small amount of polyisoprene units.*

### 2.1.2 Surfactants

For the preparation of mixed ABC/surfactant micelles, we used neutral Zonyl FSN-100 ($M_w$~950 g/mol) purchased from DuPont (Wilmington, Canada). For preparation of PIC aggregates in all cases we used cationic 1,1,2,2-tetrahydro-perfluorodecyl pyridinium chloride (HFDPCl, $M_w$~560 g/mol) obtained from the group of S. Pispas. HFDPCl was synthesized from 1H, 1H, 2H, 2H - perfluorodecyl iodide and pyridine. Structural formulae of both surfactants are in the Figure 2. HFDPCls CMC is 2.8 mM (at $T$ = 25 °C)[10].

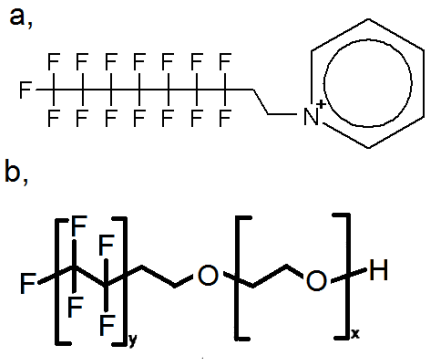


**Figure 2.** *Structural formulae of (a) cationic perfluorinated surfactant (HFDPCl) and (b) amphiphilic perfluorinated surfactant (Zonyl FSN-100)*

## *2.2 Preparation of nanoparticles*

*$PSCI_{62}$-$PEO_{259}$ (for SLS, DLS and TEM):*

20 mg of the copolymer was dissolved either in 20 ml of 0.05 M aqueous sodium tetraborate (for pH ~9) or in 20 ml of 0.1 M HCl (for pH ~1). 0.2, 0.4, 0.6, 0.8 and 1 ml of the surfactant stock solution ($c$ = 0.01 M) was added to 1 ml of the copolymer solution. Corresponding DN (%) are calculated assuming that in 0.1M HCl only sulfonic groups on the PCSI chains are ionized and all the carboxylic groups are protonated. Values are summarized in Tab. 2.

*$PSCI_{62}$-$PEO_{259}$ (for time dependence):*

Each sample was prepared by mixing 0.8 ml of copolymer solution with 0, 4, 8, 12, 14, 16, 20 and 24 µl of 0.1 M HFDPCl solution. (DN = 11, 22, 33, 39, 45, 56 and 67 %)

*$PSCI_{70}$-$PEO_{1289}$ (for SLS, DLS and TEM):*

20 mg of the copolymer was dissolved either in 20 ml of 0.05 M aqueous sodium tetraborate (for pH ~9) or in 20 ml of 0.1 M HCl (for pH ~1). Solutions were then mixed as follows: 25, 50, 75, 100, 150, 200, 250, 300 and 350 µl of surfactant solution were added into the 1 ml of the copolymer solution. Corresponding DN (%) are summarized in Tab. 2.

*PMAA-PEO:*

15 mg of the copolymer was dissolved in 15 ml of 0.05 M Sodium tetraborate. Surfactant (HFDPCl) solution was prepared by direct mixing of 56 mg of the surfactant with 1 ml of deionized water (c = 0,1 M) and again left shaken for a few minutes until it was dissolved completely. Then 10, 20, 30, 40, 50, 60, 70, 80, 90, 100, 110 and 120 µl of the surfactant solution were added to 1 ml of the copolymer solution. Corresponding DN (%) are summarized in Tab. 2.

*PCL-PEO/Zonyl FSN-100*:

The PCL-PEO solution was prepared by direct mixing of 20 mg of the copolymer with 3 ml of THF, immediate dissolution was observed (c = 1,0 g/l) followed by drop-by-drop mixing under vigorous stirring with 17 ml of distilled water. The last step of the preparation was dialysis against deionized water for total removal of THF from solution. Zonyl solution was prepared by adding 200 mg of the surfactant to a 20 ml of water (c = 10 g/l). Preparation of polymer/surfactant samples was accomplished by mixing of 1 ml of the polymer solution with 0.1, 0.2, 0.3, 0.4, 0.5, 0.6, 0.7, 0.8, 0.9 and 1 ml of the surfactant solution, so the $wt_r$ (%) polymer/surfactant mass concentration ratio varies from 1 to 10.

*$PSCI_{62}$-$PEO_{259}$ and $PSCI_{70}$-$PEO_{1289}$ (for $^{19}F$ NMR):*

Copolymer solutions were prepared by dissolving 10 mg of the copolymer in 1 ml of 0.05 M sodium tetraborate solution in $D_2O$. Surfactant solution was prepared by mixing of 56 mg of HFDPCl with 1 ml of $D_2O$. $PSCI_{62}$-$PEO_{259}$ and $PSCI_{70}$-$PEO_{1289}$ solutions were then mixed with surfactant solution so that overall apparent degree of neutralization was DN (%) = 50%.

**Table 2.** *List of samples and their apparent degree of neutralization DN (%)* [1]

| **Sample** | **1** | **2** | **3** | **4** | **5** | **6** | **7** | **8** | **9** | **10** | **11** | **12** | **13** |
|---|---|---|---|---|---|---|---|---|---|---|---|---|---|
| **$PSCI_{62}$-$PEO_{259}$** (pH = 1) | | | | | | | | | | | | | |
| DN (%) | 0 | 90 | 180 | 270 | 360 | 450 | - | - | - | - | - | - | - |
| **$PSCI_{70}$-$PEO_{1289}$** (pH = 1) | | | | | | | | | | | | | |
| DN (%) | 0 | 28 | 56 | 84 | 112 | 166 | 222 | 280 | 334 | 390 | - | - | - |
| **$PSCI_{62}$-$PEO_{259}$** (pH = 9) | | | | | | | | | | | | | |
| DN (%) | 0 | 45 | 90 | 135 | 180 | 225 | - | - | - | - | - | - | - |
| **$PSCI_{70}$-$PEO_{1289}$** (pH = 9) | | | | | | | | | | | | | |
| DN (%) | 0 | 14 | 28 | 42 | 56 | 83 | 111 | 140 | 167 | 195 | - | - | - |
| **PMAA-PEO** (pH = 9) | | | | | | | | | | | | | |
| DN (%) | 0 | 15 | 30 | 45 | 60 | 75 | 90 | 105 | 120 | 135 | 150 | 165 | 180 |
| **PCL-PEO** (pH = 7) | | | | | | | | | | | | | |
| $wt_r$ (%)[2] | 0 | 1 | 2 | 3 | 4 | 5 | 6 | 7 | 8 | 9 | 10 | - | - |

*[1] – this is not a list of all samples, only samples for SLS, DLS and TEM measurements [2] – $wt_r$ (%) is surfactant/polymer mass concentration ratio, it is not mass fraction (polymer concentration is sometimes expressed in terms of mass fraction, usually denoted as wt(%)*

## *2.3 Methods*

### 2.3.1 Light scattering measurements

The light scattering setup (ALV, Langen, Germany) consisted of a 22mW He-Ne laser operating at wavelength $\lambda$ = 632.8 nm, an ALV CGS/8F goniometer, an ALV High QE APD detector, and an ALV 5000/EPP multibit, multitau autocorrelator. Corrected excess Rayleigh ratios, $\Delta R_\theta$, and normalized time autocorrelation function of the scattered-light intensity, $g^{(2)}(t)$, were acquired at 25 °C. Measurements were performed for different scattering angles ranging from 30 to 150°.

Dynamic light scattering measurements were evaluated by fitting the measured normalized time autocorrelation function of the scattered intensity. The data were fitted with the aid of the constrained regularization algorithm (CONTIN), which provides the distribution of relaxation times $\tau$, $A(\tau)$, as the inverse Laplace transform of $g^1(t)$ function.

$$g^1(t) = \int_0^\infty A(\tau) e^{\left(\frac{-t}{\tau}\right)} d\tau \tag{11}$$

Autocorrelation functions providing monomodal relaxation time distributions by the CONTIN method were further fitted to the second-order cumulant expansion,

$$\ln g^1(t) = -\Gamma_1 t + \frac{\Gamma_2}{2} t^2 \tag{12}$$

where $\Gamma_1$ and $\Gamma_2$ are the first and the second moments of the distribution function of relaxation rates. The diffusion coefficient of the particles can be evaluated by the extrapolation of $\Gamma_1/q^2$ using equation,

$$\frac{\Gamma_1(q,c)}{q^2} = D\left(1 + CR_g{}^2 q^2 + k_D c\right) \tag{13}$$

where $k_D$ is the hydrodynamic virial coefficient and $C$ is the structural parameter reflecting the shape, polydispersity, and internal dynamics of the scattering particles.

### 2.3.2 Transmission electron microscopy measurements

TEM micrographs were obtained with Tecnai G2 Spirit Twin 12 microscope operated at 120 kV. A small amount of the solution was sputtered onto a TEM copper grid covered with thin carbon film, which was left to evaporate at room temperature and then observed in the microscope. The samples were not stained. Sufficient contrast in the micrographs was obtained using a combination of a sensitive TEM CCD camera (Morada, Olympus) and a small objective aperture (20 or 40 μm).

### 2.3.3 Cryogenic transmission electron microscopy

3 μL of the sample solution was applied to an electron microscopy grid covered with perforated carbon supporting film (C-flat 2/2-2C, Electron Microscopy Science) glow discharged for 20s with 10mA current. Most of the sample was removed by blotting (Whatman no. 1 filter paper) for approximately 1 s, and the grid was immediately plunged into liquid ethane held at –183 ºC. The sample was then transferred without rewarming into a Tecnai Sphera G20 electron microscope using a Gatan 626 cryo-specimen holder. The images were recorded at 120 kV accelerating voltage and microscope magnification ranging from 5000× to 14 500× using a Gatan UltraScan 1000 slow scan CCD camera (giving a final pixel size from 2 to 0.7 nm) and low dose mode with the electron dose not exceeding 1500 electrons per $nm^2$. Typical value of applied under focus ranged between 1.5 to 2.7 μm. The applied blotting conditions resulted in the specimen thickness varying between 100 to cca. 300 nm.

### 2.3.4 Nuclear magnetic resonance

$^{19}F$ NMR spectra were recorded on a Varian 300 spectrometer at 25 ºC.

# 3. Results and discussion

Double hydrophilic block copolymers are in most cases readily water soluble. Usually, depending on the structure of the copolymer, it takes between a few seconds to hours of stirring. In our case, PSCI-PEO and PMAA-PEO copolymers dissolved in sodium tetraborate and in 0.1 M HCl as well after a few minutes. On the other hand, amphiphilic PCL-PEO is not soluble in pure water. In that case, the copolymer is usually dissolved in a common solvent e.g. that is good for both blocks. This common solvent can be prepared by mixing two different solvents, i.e. organic solvent and water or it may be only one solvent, as usual. We couldn't directly dissolve PCL-PEO copolymers in water so we used THF, which is a common solvent for both PCL and PEO.

## *3.1 $PSCI_{62}$-$PEO_{259}$*

### 3.1.1 Particles prepared in 0.1 M HCl

*SLS and DLS* measurements (Fig. 3 and Fig. 4) showed that the prepared particles are not larger than 60 nm regardless of how much surfactant was added to the copolymer solution. It is obvious, that even before addition of any amount of the surfactant there are particles with the radius of about 20 nm in the copolymer solution. This is probably because of the presence of hydrophobic PI units, what causes that PSCI chain is not soluble enough and copolymer has an amphiphilic character. We can still see an increase in size after "partial neutralization" (DN (%) = 90) to around $R_h$ ~ 35 nm. After addition of higher amount of surfactant, particles broke up to form structures not larger than 30 nm.

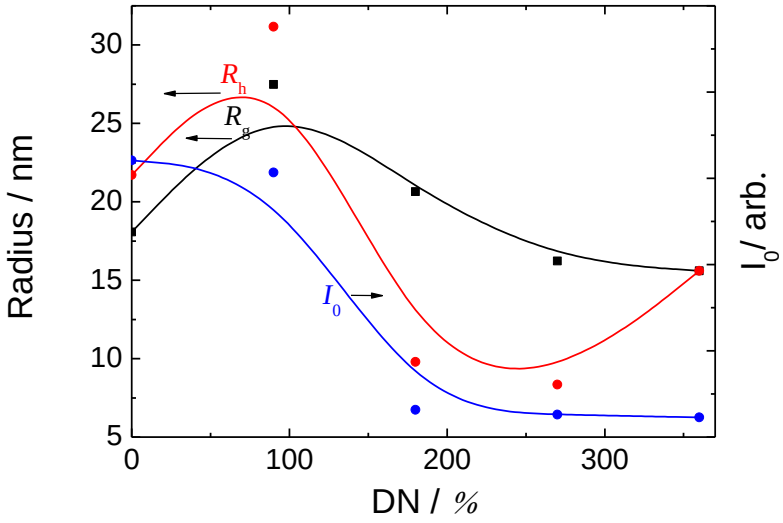


**Figure 3.** *Effect of added surfactant, expressed in DN(%), to the 1 ml of 1g/l copolymer solution, on the hydrodynamic radius, $R_h$, radius of gyration, $R_g$, and the scattering intensity at the zero scattering angle, $I_0$, of the aggregates of $PSCI_{62}$-$PEO_{259}$ with the surfactant, obtained from DLS and SLS measurements. In 0.1 M HCl.*

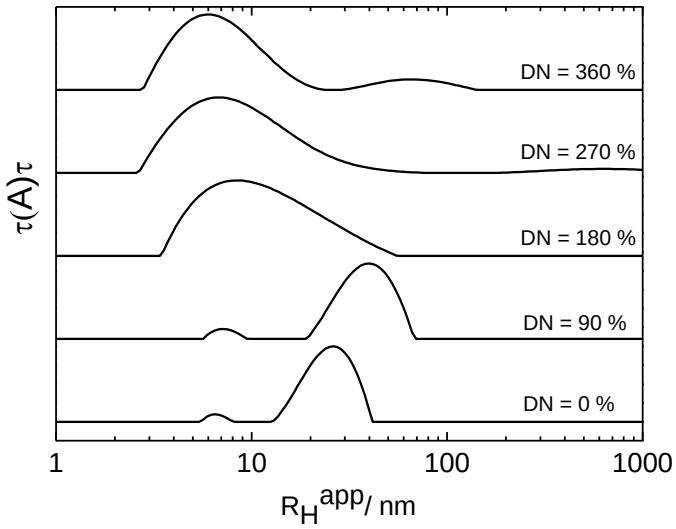


**Figure 4.** *Unweighted hydrodynamic radius distributions obtained at the scattering angle θ=90° by DLS of $PSCI_{62}$-$PEO_{259}$/HFDPCl, as a function apparent degree of neutralization, DN (%), indicated on the right side above each curve. In 0.1 M HCl.*

TEM micrograph (Fig. 5) shows spherical particles of the average radius corresponding to that obtained from DLS measurements.

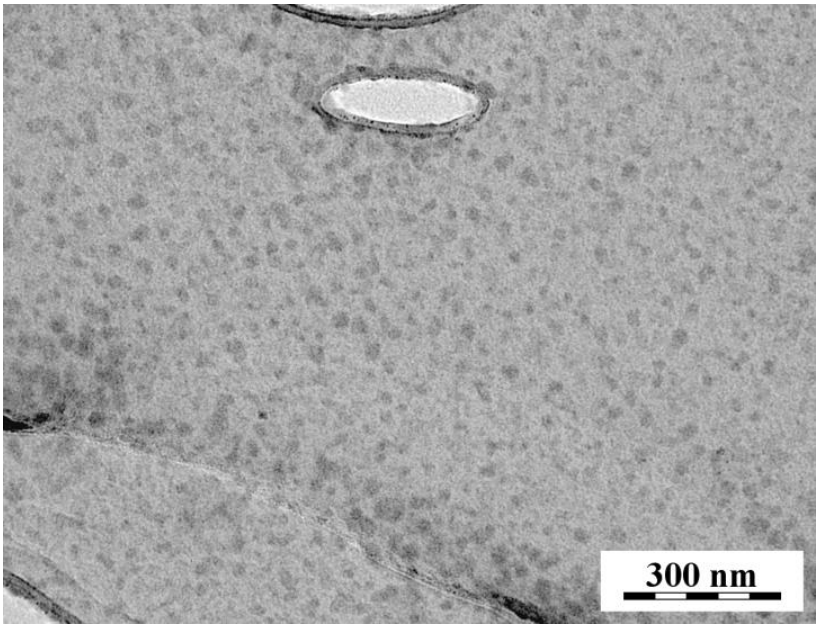


**Figure 5**. *TEM image of $PSCI_{62}$-$PEO_{259}$ PIC particles in 0.1 M HCl, for apparent degree of neutralization DN = 90 %.*

### 3.1.2 Particles prepared in 0.05 M sodium tetraborate buffer

It is obvious that in alkaline solutions, both (i.e. COOH and $SO_3H$) groups are deprotonated. In such conditions, polyelectrolyte chains of the copolymer should be more water soluble but also more stretched than in acidic solution (because of high negatively charged groups repulsion). As in the case of the solution at pH 1, there are particles formed in the pure copolymer solution sample with no surfactant added but the particles are much larger while the scattering intensity is comparable to that in acidic solution, which indicates that the particles are looser. After addition of the surfactant, the decrease in the particle size is observed. This may be explained by the collapse of aggregates polyelectrolyte cores as a result of decrease in repulsion between neighboring negatively charged groups after PSCI chain "neutralization". Addition of higher amounts of surfactant caused aggregates to slightly increase their radius of gyration, while the hydrodynamic radius increased steeply. The more surfactant was added, the stronger was the tendency to aggregate and form polydisperse mixtures of aggregates (see Fig. 7). *Cryo*-TEM (Fig. 9) revealed that at

DN = 50 %, copolymer assemblies formed wormlike micelles, with tendency to associate (Fig. 9c).

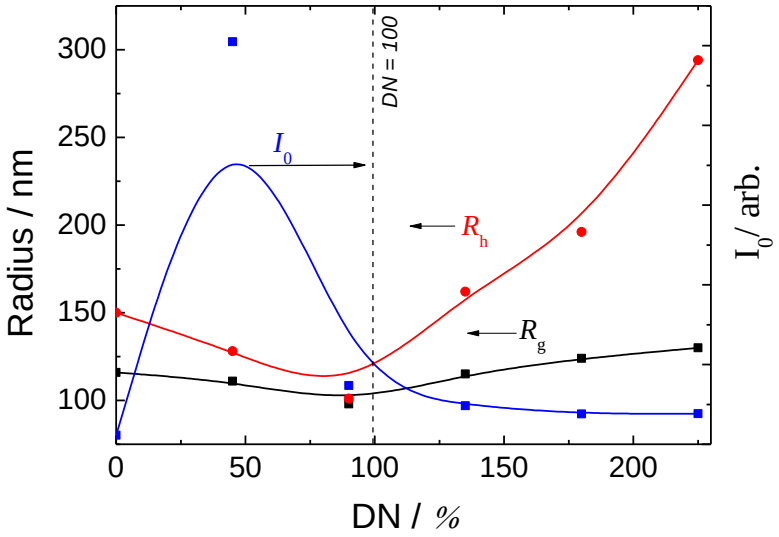


**Figure 6.** *Effect of added surfactant to the 1 ml of 1 g/l copolymer solution, on the hydrodynamic radius, $R_h$, radius of gyration, $R_g$, and scattering intensity for zero angle $I_0$, of the aggregates of $PSCI_{68}$-$PEO_{259}$ with the surfactant, obtained from DLS and SLS measurements. In 0.05 M $Na_2B_4O_7$.*

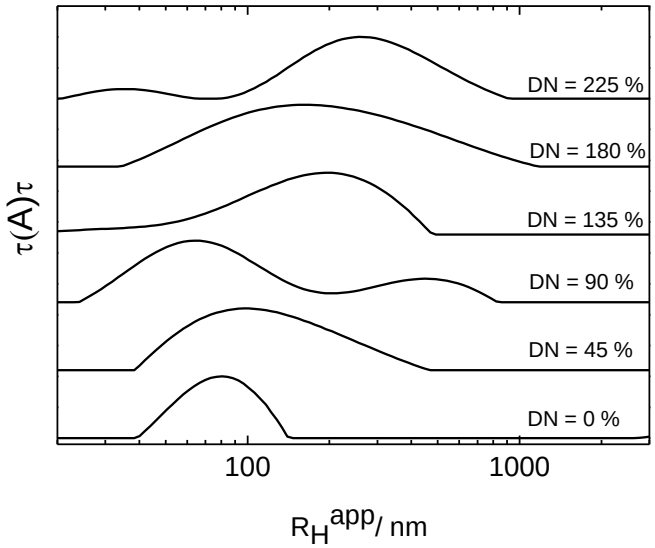


**Figure 7.** *Unweighted hydrodynamic radius distributions obtained at the scattering angle $\theta$ = 90 ° by DLS for $PSCI_{62}$-$PEO_{259}$/HFDPCl aggregates, as a function of apparent degree of neutralization, DN (%) indicated on the right side above each curve.*

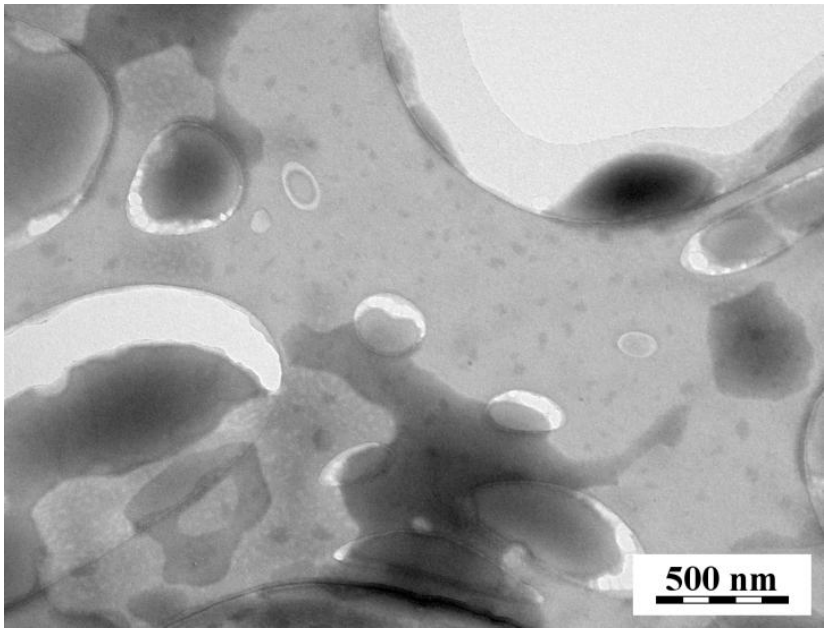


**Figure 8**. *TEM measurement of $PSCI_{62}$-$PEO_{259}$ PIC particle aggregates in 0.05 M Sodium tetraborate buffer for apparent degree of neutralization DN = 90 %.*

Hydrodynamic radius distributions (Fig.7) and TEM measurements (Fig. 8) proved high polydispersity and instability of the samples, and raised the question of the kinetics of aggregates formation. That is also why we prepared another set of samples for stability measurements (see chapter 2.2 for the samples preparation description). Light scattering measurements have been performed directly after samples preparation, i.e. after 1 hour and repeated after 2 hours, 3 days and 2 weeks. As expected, the radius of gyration changed with time (Fig. 10).

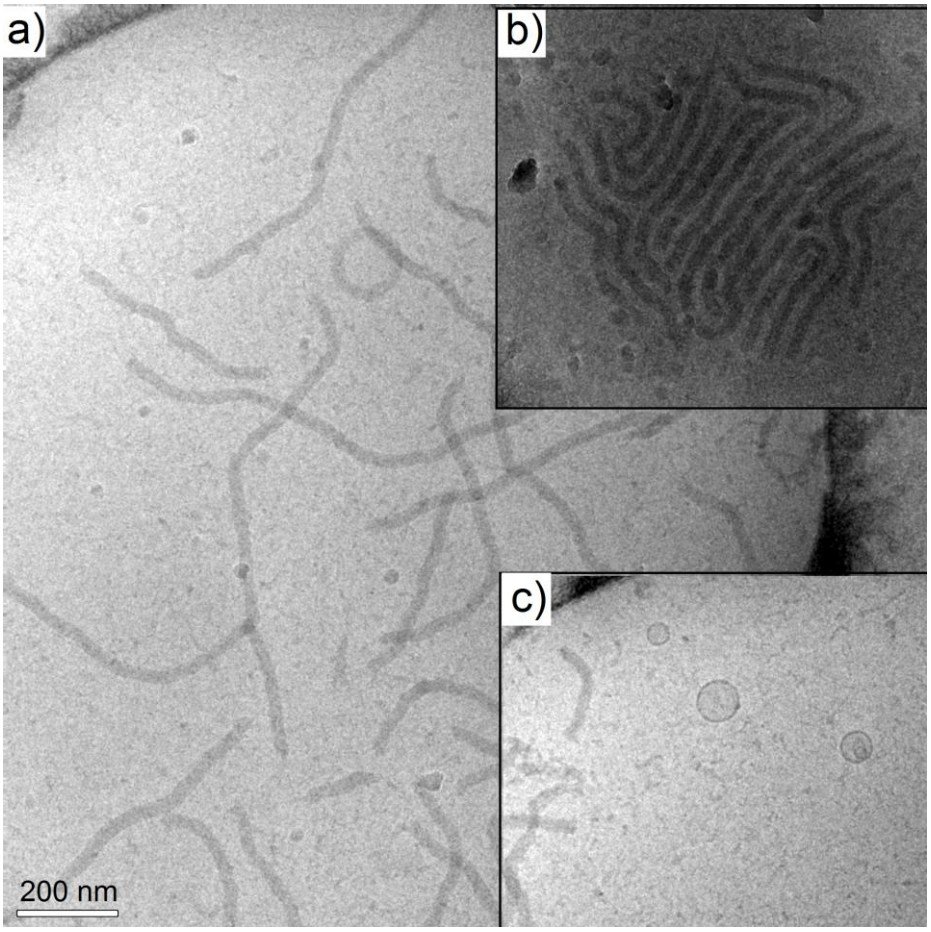


**Figure 9**. *cryo-TEM measurement of $PSCI_{62}$-$PEO_{259}$ PIC particle aggregates in 0.05 M Sodium tetraborate buffer for apparent degree of neutralization DN = 50 %. a) worms, b) associated worms, c) PIC worms and HFDPCl vesicles coexisting.*

From Fig. 10 we can see that radius of gyration significantly changed its value especially for samples with the apparent neutralization ratios 35 and 41 %. Therefore in order to achieve particles formed from such copolymers to be relatively stable, we need to let them self-assemble at least for a few days.

*Cryo*-TEM appears to be more useful then TEM measurements. Unfortunately we managed to obtain only images for $PSCI_{62}$-$PEO_{259}$ and $PSCI_{70}$-$PEO_{1289}$ in sodium tetraborate buffer. Figure 9 shows that interaction of HFDPCl with *$PSCI_{62}$-$PEO_{259}$* is not strong enough to ensure 100% mixing in. Even for the sample with DN = 50%, surfactant vesicles and copolymers worms coexisted together in solution.

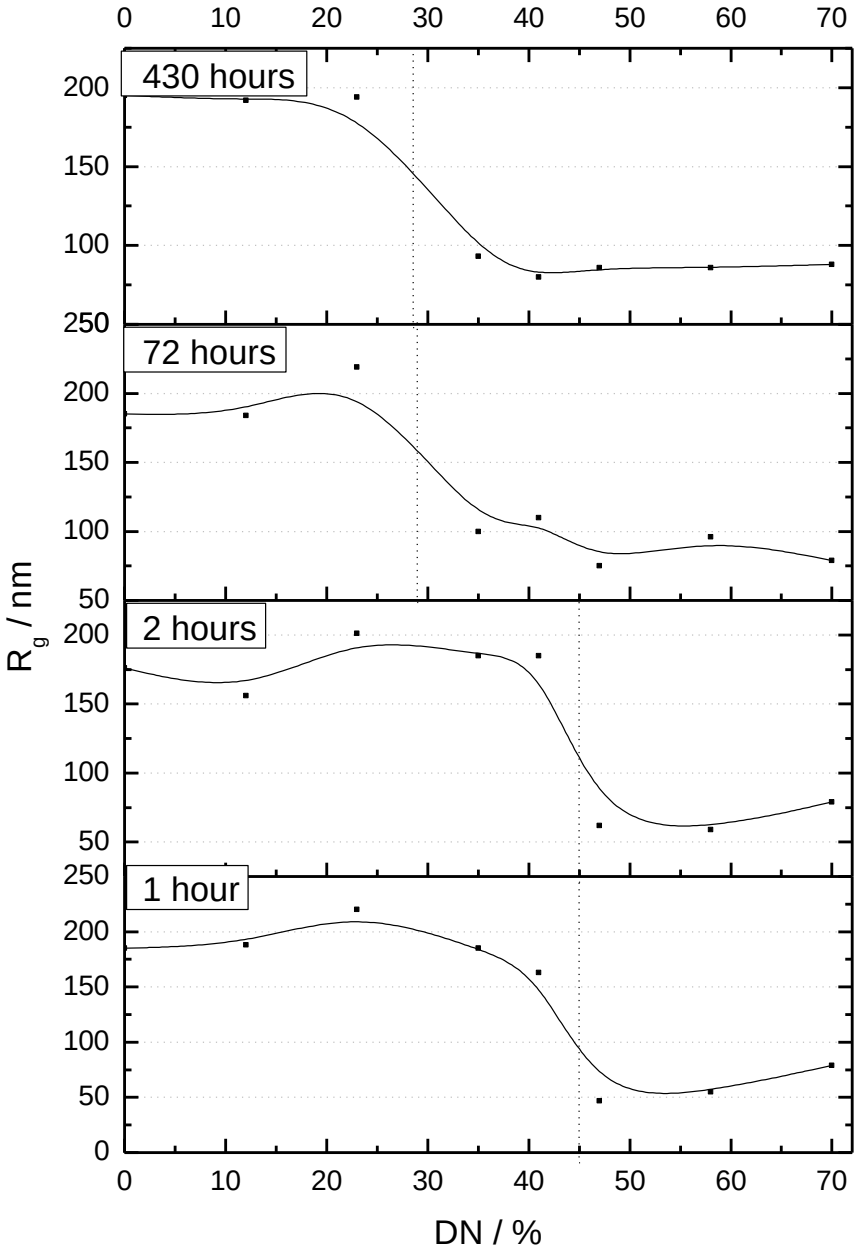


**Figure. 10** *Four light scattering measurements of the PIC formed by $PSCI_{62}$-$PEO_{259}$ copolymer (in 0.05 M Sodium tetraborate buffer) 1, 2, 72 and 430 hours after mixing with the surfactant and their radius of gyration as a function of the surfactant concentration (DN = 0, 12, 23, 35, 41, 47, 58 and 70 %).*

## *3.2 $PSCI_{70}$-$PEO_{1289}$*

### 3.2.1 Particles prepared in 0.1 M HCl

As expected, $PSCI_{70}$-$PEO_{1289}$ PIC aggregates at pH ~ 1 without the presence of the surfactant were larger than $PSCI_{62}$-$PEO_{259}$ ones. Fig. 11 and Fig. 12 show, that in contrast to $PSCI_{62}$-$PEO_{259}$ PIC particles at pH ~ 1, where the particles disrupted after the addition of a higher amount of the surfactant, here we can still see the scattering from particles of the hydrodynamic radius around 80 nm. It`s probably because of the increased PEO chain length which causes a better solvation of hydrophobic polyelectrolyte cores of the particles and increases their water solubility and stability.

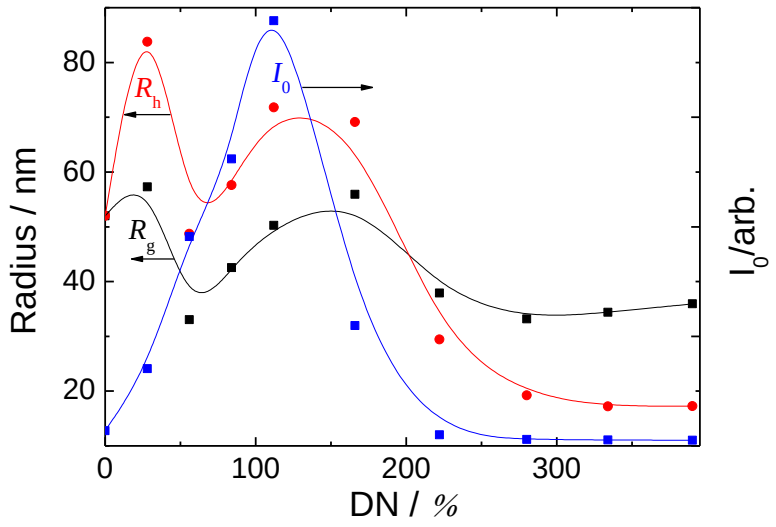


**Figure 11.** *Effect of added surfactant to the 1 ml of 1g/l copolymer solution in 0.1 M HCl, on the hydrodynamic radius, $R_h$, radius of gyration, $R_g$, and scattering intensity for the zero angle scattering intesity, $I_0$, of the aggregates of $PSCI_{70}$-$PEO_{1259}$ with HFDPCl, obtained from DLS and SLS measurements as a function of DN(%). In 0.1 M HCl.*

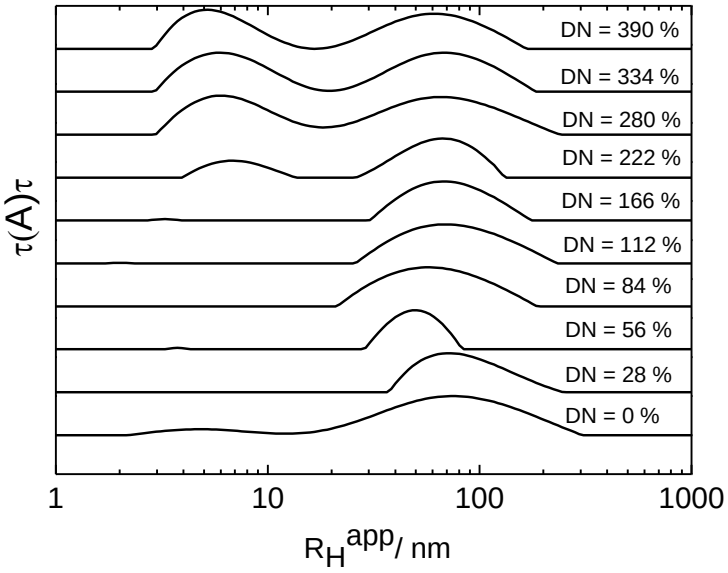


**Figure 12.** *Unweighted hydrodynamic radius distributions obtained at the scattering angle θ = 90° by DLS of $PSCI_{70}$-$PEO_{1289}$/HFDPCl, for various apparent degree of neutralization ratios, DN (%). In 0.1 M HCl.*

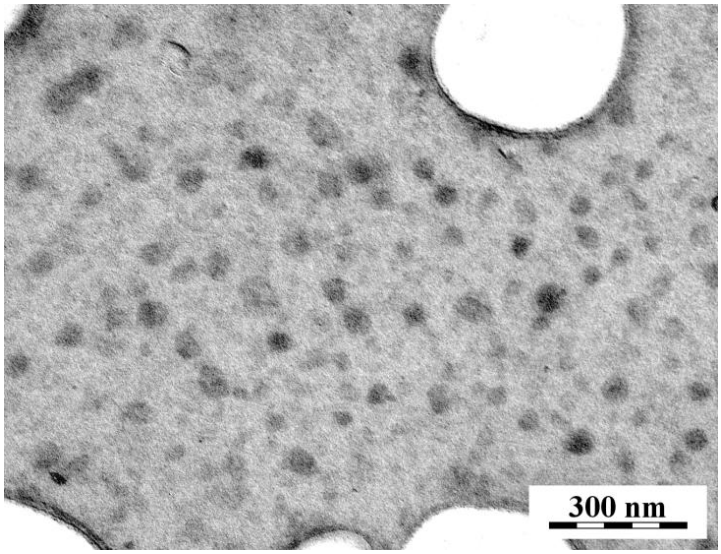


**Figure 13.** *TEM image of $PSCI_{70}$-$PEO_{1289}$ PIC particle aggregates in 0.1 M HCl for the apparent degree of neutralization, DN = 166 %.*

### 3.2.2 Particles prepared in 0.05 M Sodium tetraborate buffer

Similarly to $PSCI_{62}$-$PEO_{259}$/HFDPCl particles prepared in sodium tetraborate buffer, $PSCI_{70}$-$PEO_{1289}$/HFDPCl particles in sodium tetraborate buffer exhibit strong tendency to form polydisperse aggregates with increasing amount of the surfactant added (obvious from Fig. 15 and Fig 16). Figure 14 shows increasing hydrodynamic and gyration radii. The decrease of the size in the DN range from 14 to 56 % is evident. It is again caused by decreasing repulsion of negatively charged polyelectrolyte groups with increasing apparent degree of neutralization, which leads to the collapse of the cores.

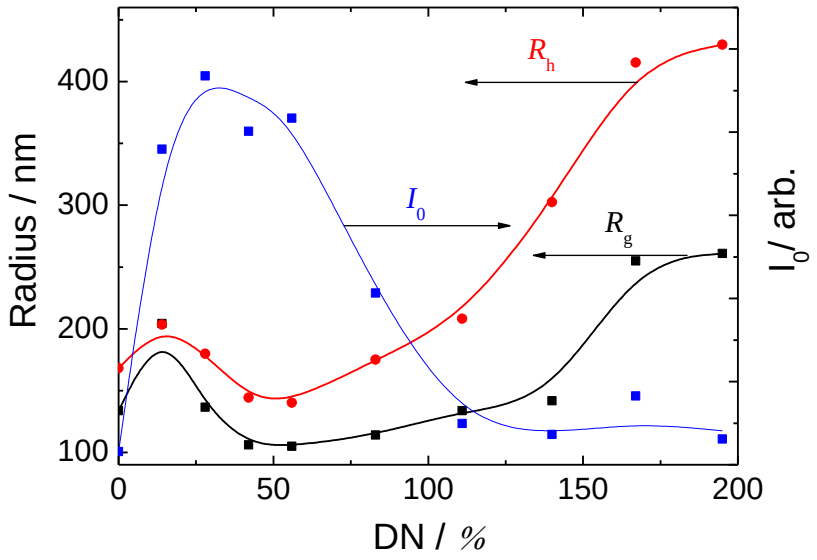


**Figure 14.** *Effect of added surfactant to the 1 ml of 1g/l copolymer solution in 0.05 M $Na_2B_4O_7$, on the hydrodynamic radius, $R_h$, radius of gyration, $R_g$, and the zero angle scattering intensity, $I_0$, ,of the aggregates of $PSCI_{70}$-$PEO_{1289}$ with HFDPCl, obtained from DLS and SLS measurements, as a function of DN(%).*

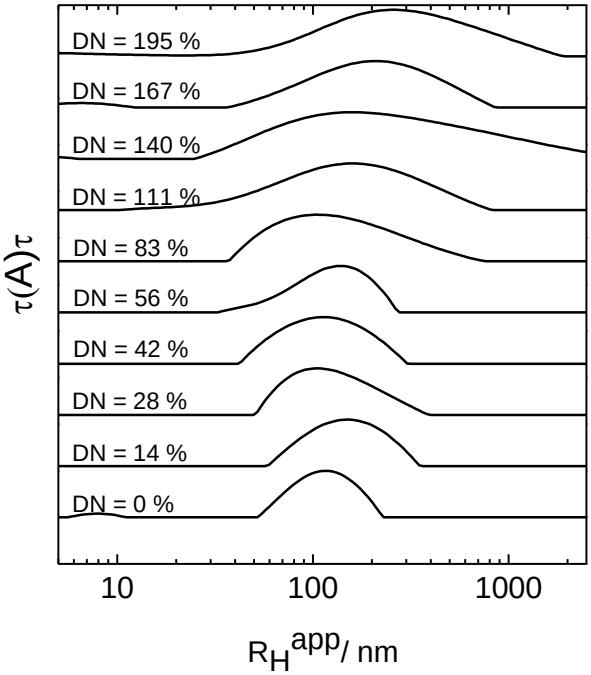


**Figure 15.** *Unweighted hydrodynamic radius distributions obtained at the scattering angle θ = 90° by DLS of $PSCI_{70}$-$PEO_{1289}$/HFDPCl, for various apparent degree of neutralization ratios, DN (%).*

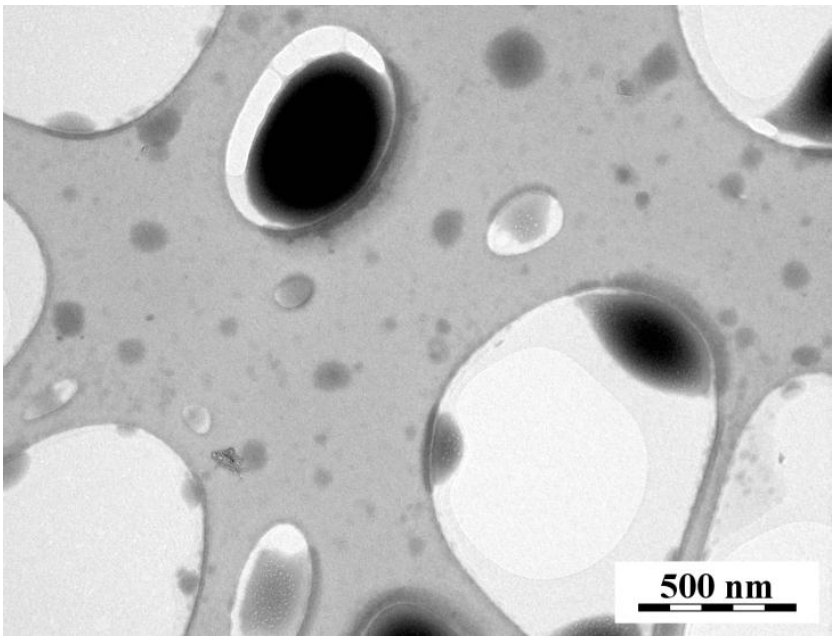


**Figure 16**. *TEM measurement of $PSCI_{70}$-$PEO_{1289}$ PIC particle aggregates in 0.05 M Sodium tetraborate buffer for apparent degree of neutralization DN = 56 %.*

*Cryo*-TEM showed that $PSCI_{70}$-$PEO_{1289}$ PIC micelles formed globular micelle aggregates (Fig. 17), instead of wormlike micelles of $PSCI_{62}$-$PEO_{259}$. Again, the coexistence of surfactant vesicles and copolymer micelles was proven. In this case there were even more vesicles present.

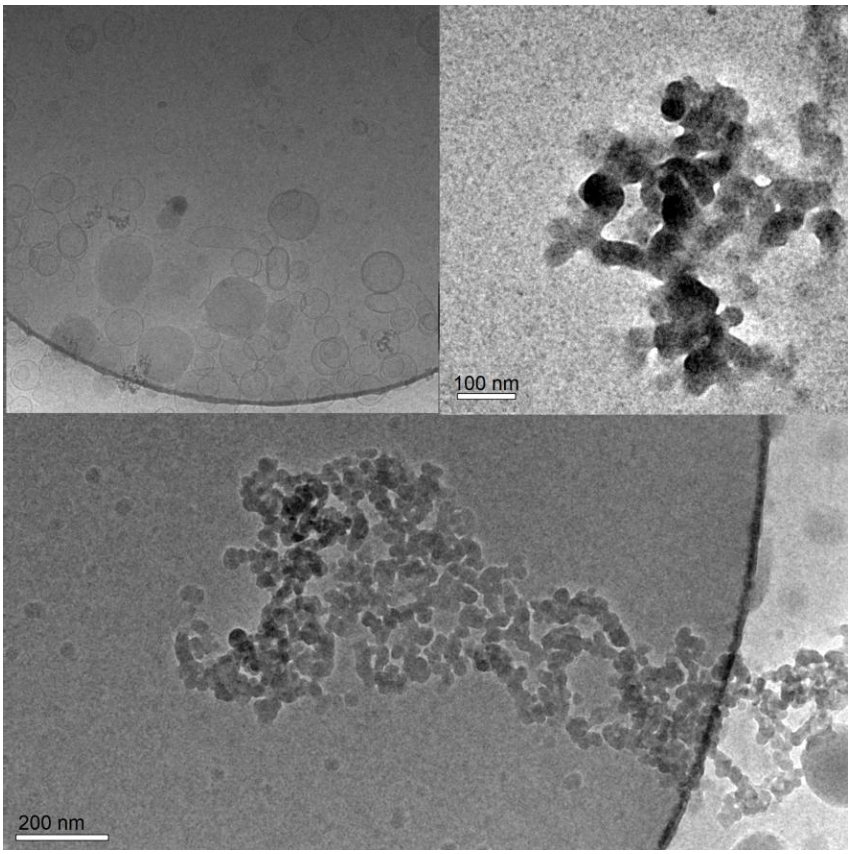


**Figure 17**. *Cryo-TEM image of $PSCI_{70}$-$PEO_{1289}$ PIC particle aggregates in 0.05 M Sodium tetraborate buffer for apparent degree of neutralization DN = 50 %.*

## *3.3 PMAA-PEO*

Copolymer solutions were transparent before mixing with the surfactant and became turbid after mixing. For the first six consecutive DN ratios, it was possible to visually relate turbidity to the amount of the surfactant added. Though the scattering intensity increased, light scattering experiments showed decrease in the radius of gyration and hydrodynamic radius (especially in DN range from 15 to 90 %), see Fig.18. Light

scattering experiments also showed particles to have the lowest polydispersity in the sample with apparent neutralization degree of DN = 75%, see Fig. 19. This phenomenon is expected to occur when DN = 100%.

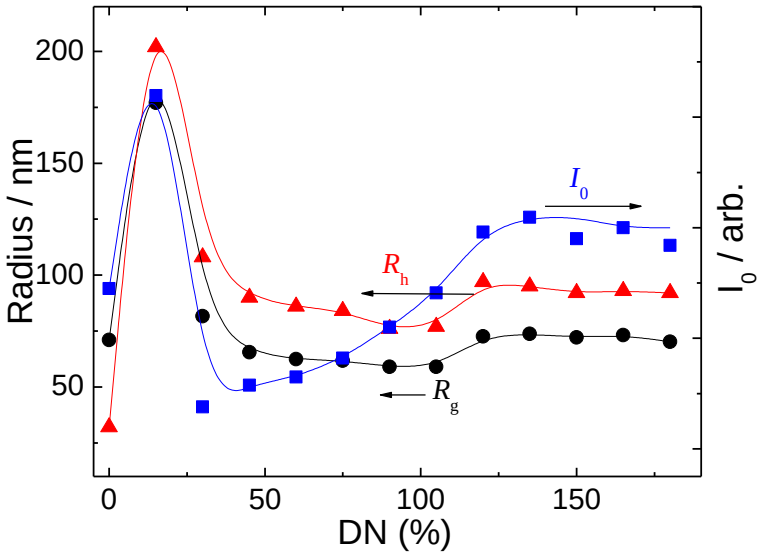


**Figure 18**. *Radii of nanoaggregates obtained for $PMAA_{477}$-$PEO_{698}$ / HFDPCl different apparent degrees of neutralization, DN (%), of the complexes by DLS and SLS. $R_h$ – mean hydrodynamic radius, $R_g$ – mean radius of gyration, $I_0$ – scattering intensity for zero angle, of the aggregates.*

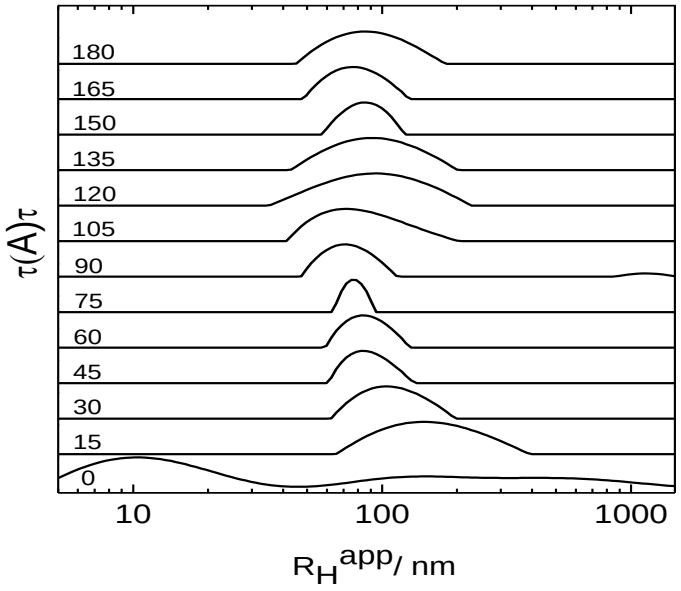


**Figure 19.** *Unweighted hydrodynamic radius distributions obtained at the scattering angle $\theta$ = 90° by DLS for different $PMAA_{477}$-$PEO_{698}$/HFDPCl apparent degree of neutralization, DN (%), (indicated above the corresponding curves).*

PMAA-PEO copolymers didn't form such large aggregates (Fig. 19) as it was obvious for both PSCI-PEO copolymers, after addition of an excess of the surfactant (Figs .7 and 15). This difference may be caused by unmodified isoprene units that are present in PSCI chains which promoted aggregation of the PSCI block due to attractive hydrophobic interactions.

### *3.4 Amphiphilic PCL-PEO/Zonyl aggregates*

Both DLS and SLS measurements (Figs. 20 and Fig. 21) showed a large initial increase in the size of the aggregates and their scattering intensity, followed by a less steep growth of $R_g$, $R_h$ and $I_0$. Surfactant/copolymer interaction and potential self-assembly of amphiphilic PCL-PEO and neutral Zonyl FSN-100 (CMC = 0.011 mM) is based upon hydrophobic interactions.

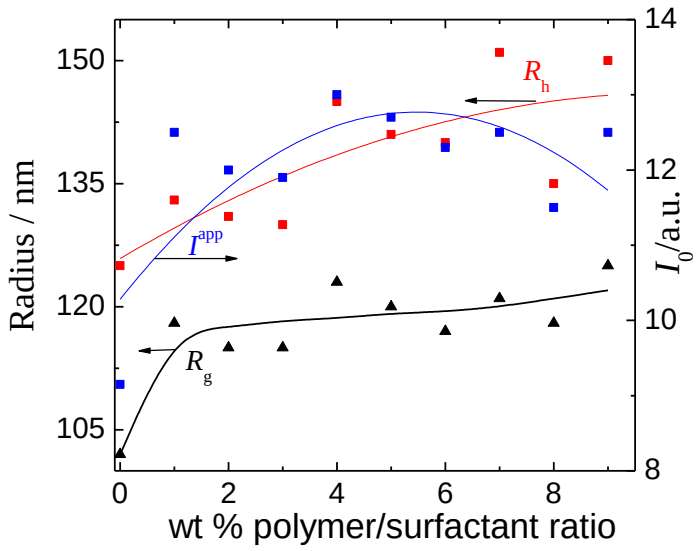


**Figure 20**. *LS data of nanoaggregates obtained for different $PCL_{281}$-$PEO_{114}$/Zonyl FSN-100 mass concentration ratios, α, in water determined by DLS and SLS. $R_h$ – mean hydrodynamic radius, $R_g$ – mean radius of gyration, $I_0$ – scattering intensity for zero scattering angle.*

The LS measurements showed only slight changes in the scattering behavior of the system. Since we have not carried out TEM measurements so far, it's hard to deduce more about their interaction and possible self-assembly. In order to do so, it is necessary to do further experimental investigation of the system.

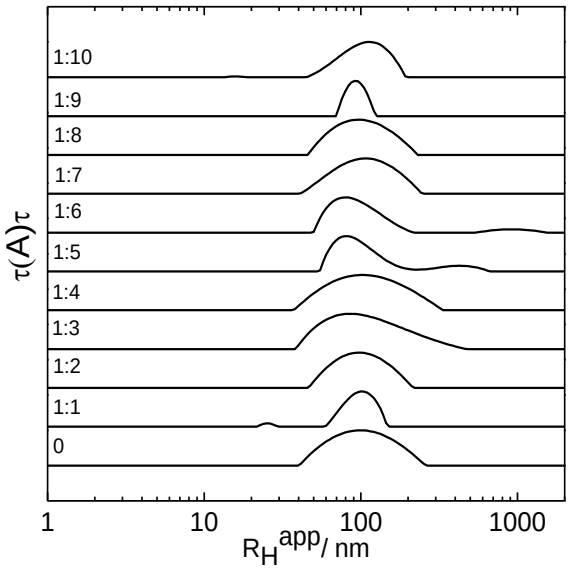


**Figure 21**. *Unweighted hydrodynamic radius distributions obtained at the scattering angle $\theta$ = 90° by DLS for different $PCL_{281}$-$PEO_{114}$/surfactant weight ratios (indicated above the corresponding curves).*

## *3.5 NMR measurements*

The most important properties of our self-assembled particles with respect to their potential use as $^{19}$F NMR contrast agents are of course those related to magnetic resonance such as signal-to-noise ratio (SNR, dependent on the $^{19}$F nuclei content of the nanoaggregates and their environment), chemical shifts, $T_1$ (the spin-lattice relaxation time) and $T_2$ (the spin-spin relaxation time). $^{19}$F NMR spectra we obtained are in Fig. 22, Fig. 23 and Fig. 24 from which it is easy to see their different appearances.

Obviously the SNR is lower in the $PSCI_{70}$-$PEO_{1259}$ nanoparticles which contain less $^{19}$F as compared with $PSCI_{62}$-$PEO_{289}$ or even with pure surfactant solution. From Fig. 22, that was obtained from pure perfluorosurfactant with concentration of around 0.1 M (1.7 M of $^{19}$F nuclei), it is possible to easily detect multiplets. Decrease of $^{19}$F nuclei concentration to ~ 0.034 M (cca. 50 times) rapidly worsened spectra quality, see Fig. 23.

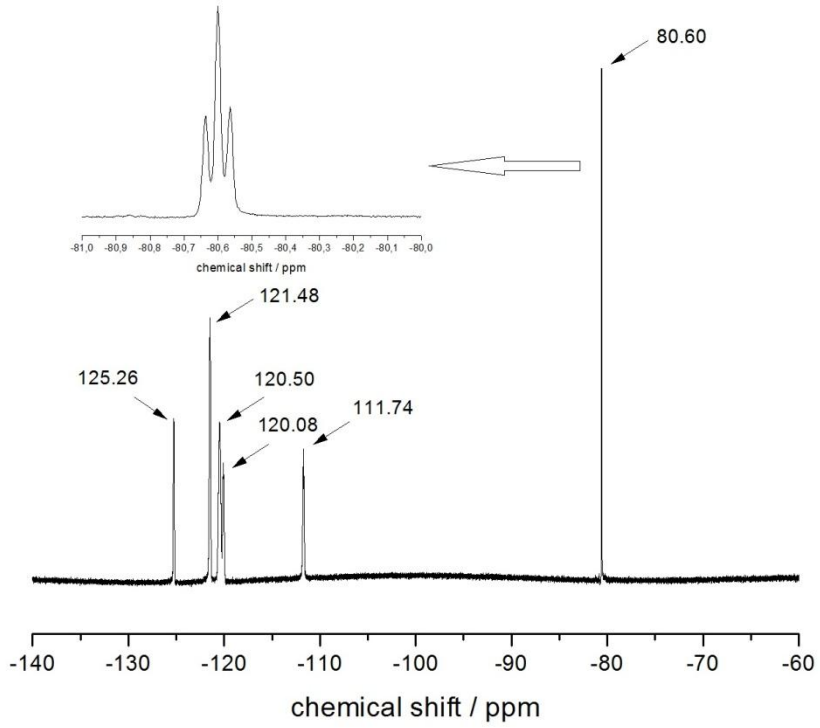


**Figure 22.** *$^{19}F$ NMR spectra of pure concentrated HFDPCl solution*

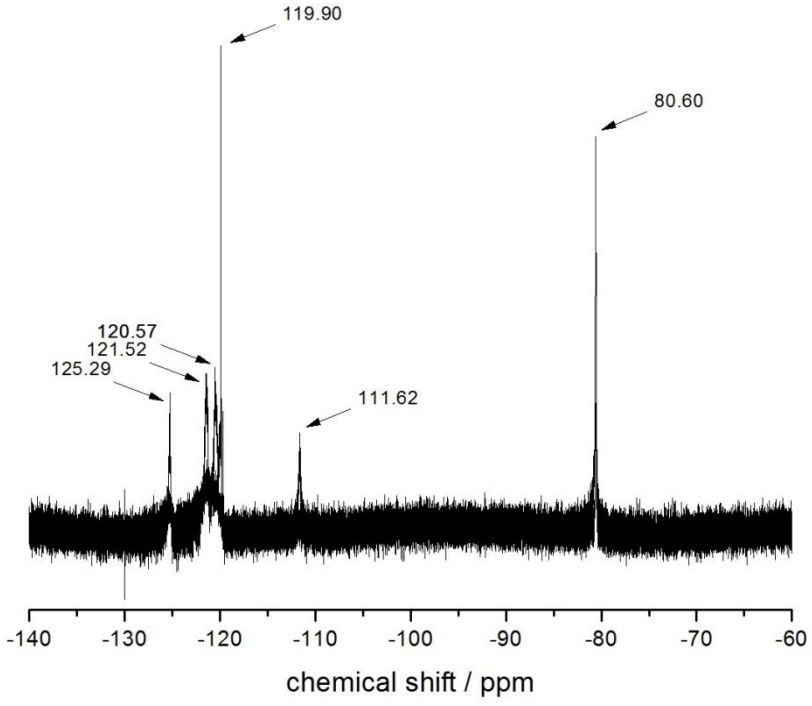


**Figure 23. .** *$^{19}F$ NMR spectra of $PSCI_{62}$-$PEO_{289}$/HFDPCl nanoaggregates*

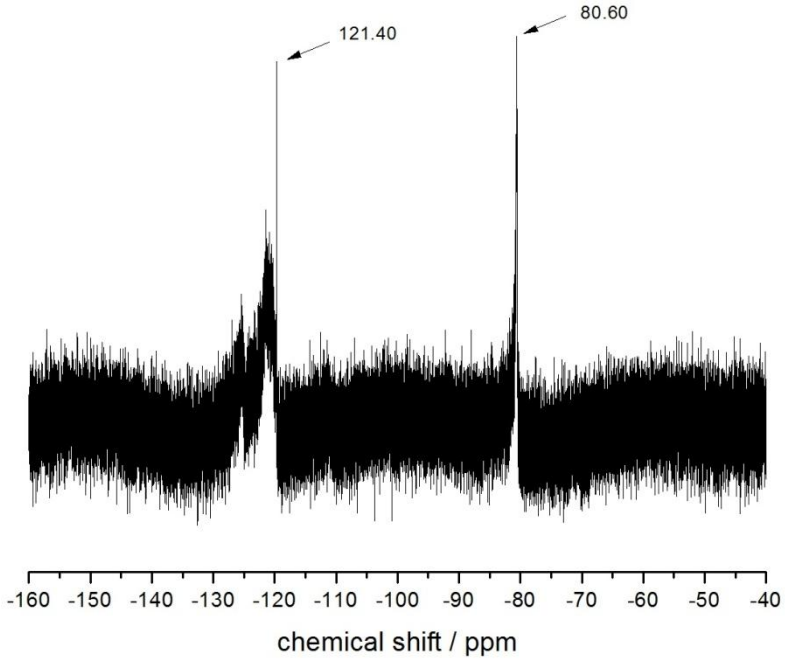


**Figure 24. .** *$^{19}$F NMR spectra of PIC $PSCI_{70}$-$PEO_{1259}$/HFDPCl nanoaggregates*

Further decrease in $^{19}$F nuclei concentration (cca 100 times) to 0.017 M caused spectra to become of poor quality. This indicates that particles present in tissue in this concentration, wouldn't give signal that is strong enough to be useful.

# 4. Conclusion

The purpose of elaboration of this thesis was mainly to compare several double hydrophilic block copolymers forming complexes with perfluorinated surfactants. On the basis of the obtained results we can conclude that PIC particles properties such as radius of gyration, polydispersity or hydrodynamic radius (aside from structural factors of the copolymer and the surfactant) are strongly dependent on the copolymer/surfactant concentration ratio.

It is also important to point out that in relation to the copolymers structure (i.e. long polymeric chains) we have to think about particles formation kinetics. Such self-assemblies may change their arrangement during at least few hours, days or even weeks, in order to adopt the most stable structure. This is evident from Fig. 10. When comparing Fig. 3 with Fig. 6 and Fig. 11 with Fig. 14, we clearly see that pH of the

solution also significantly influences the properties of the particles. Questionable is to what extent the polyion chain can form complex with the fluorosurfactants. Fig. 9 shows that even in the sample with the apparent degree of neutralization as low as 50 %, we can see the fluorosurfactants vesicles coexisting with the copolymer aggregates (also in Fig. 17).

The results of PMAA-PEO measurements were similar to the results obtained by Bronich et al.[18], who used N-alkylpyridinium cations as the surfactant. This corroborated the hypothesis that there is a kind of general behavior of double hydrophilic polyelectrolyte/surfactant self-assemlies. PMAA-PEO in sodium tetraborate buffer showed a higher stability and lower polydispersity in comparison with both PSCI-PEO copolymers (especially at DN = 75 %) as it is evident from Fig. 15 and Fig. 19. In excess of the surfactant, PMAA-PEO particles also had stable smaller hydrodynamic radii, which may be caused by a higher compactness of PMAA-PEO particles. On the other hand, PSCI-PEO in excess of the surfactant had a tendency to increase its hydrodynamic radius and form loose polydisperse aggregates. PSCI-PEO nanoaggregates in 0.1 M HCl (~ pH = 1) were much smaller ($R_g$ = 25 – 50 nm) and in excess of the surfactant tend to break down to even smaller particles.

The low SNR of the samples could be a weakness of the fluorine PIC copolymer/surfactant nanoparticles application potential. For example, for $^{19}$F MRI to produce an image quality similar to that of $^{1}$H MRI, whose signal derives from nearly two-thirds of all nuclei present in the body, nanoparticles require a very high density of $^{19}$F nuclei (in addition to a high tissue concentration). When thinking about problems related to achieving a high tissue concentration, we should point out, that even though long hydrophilic PEO chains improve nanoparticles stability, they significantly increase nanoparticles hydrodynamic radius (by corona thickening) and reduce concentration of $^{19}$F in nanoparticles (as long as PEO corona doesn’t contain surfactant at all).

The measurements done on amphiphilic PCL-PEO with neutral Zonyl FSN-100 surfactant showed only a slight increase of the radius of gyration of the particles and their hydrodynamic radius after mixing. The preparation of amphiphilic block

copolymer/surfactant mixed micelles formed without the contribution of electrostatic attractive interactions may appear to be much more complicated than in the case of PIC aggregates (especially for surfactant concentrations exceeding the CMC of the surfactant) and a further research is required, in order to obtain more information about its behavior.

# 5. References


1. Ruiz-Cabello, J.; Barnett, B. P.; Bottomley, P. A.; Bulte, J. W. M., Fluorine ((19)F) MRS and MRI in biomedicine. *NMR in Biomedicine* **2011,** 24, (2), 114-129.
2. Gerig, J. T., FLUORINE NUCLEAR-MAGNETIC-RESONANCE OF FLUORINATED LIGANDS. *Methods in Enzymology* **1989,** 177, 3-23.
3. Danielson, M. A.; Falke, J. J., Use of F-19 NMR to probe protein structure and conformational changes. *Annual Review of Biophysics and Biomolecular Structure* **1996,** 25, 163-195.
4. Yu, J. X.; Kodibagkar, V. D.; Cui, W. N.; Mason, R. P., F-19: A versatile reporter for non-invasive physiology and pharmacology using magnetic resonance. *Current Medicinal Chemistry* **2005,** 12, (7), 819-848.
5. Pan, D. P. J.; Caruthers, S. D.; Chen, J. J.; Winter, P. M.; SenPan, A.; Schmieder, A. H.; Wickline, S. A.; Lanza, G. M., Nanomedicine strategies for molecular targets with MRI and optical imaging. *Future Medicinal Chemistry* **2010,** 2, (3), 471-490.
6. Kaneda, M. M.; Caruthers, S.; Lanza, G. M.; Wickline, S. A., Perfluorocarbon Nanoemulsions for Quantitative Molecular Imaging and Targeted Therapeutics. *Annals of Biomedical Engineering* **2009,** 37, (10), 1922-1933.
7. Tran, T. D.; Caruthers, S. D.; Hughes, M.; Marsh, J. N.; Cyrus, T.; Winter, P. M.; Neubauer, A. M.; Wickline, S. A.; Lanza, G. M., Clinical applications of perfluorocarbon nanoparticles for molecular imaging and targeted therapeutics. *International Journal of Nanomedicine* **2007,** 2, (4), 515-526.
8. Peng, H.; Blakey, I.; Dargaville, B.; Rasoul, F.; Rose, S.; Whittaker, A. K.,

Synthesis and Evaluation of Partly Fluorinated Block Copolymers as MRI Imaging Agents. *Biomacromolecules* **2009,** 10, (2), 374-381.

9. Imae, T., Fluorinated polymers. *Current Opinion in Colloid & Interface Science* **2003,** 8, (3), 307-314.
10. Matsuoka, K.; Moroi, Y., Micellization of fluorinated amphiphiles. *Current Opinion in Colloid & Interface Science* **2003,** 8, (3), 227-235.
11. Srinivas, M.; Heerschap, A.; Ahrens, E. T.; Figdor, C. G.; de Vries, I. J. M., (19)F MRI for quantitative in vivo cell tracking. *Trends in Biotechnology* **2010,** 28, (7), 363-370.
12. Shiraishi, K.; Kawano, K.; Maitani, Y.; Yokoyama, M., Polyion complex micelle MRI contrast agents from poly(ethylene glycol)-b-poly(L-lysine) block copolymers having Gd-DOTA; preparations and their control of T(1)-relaxivities and blood circulation characteristics. *Journal of Controlled Release* **2010,** 148, (2), 160-167.
13. Nasongkla, N.; Bey, E.; Ren, J. M.; Ai, H.; Khemtong, C.; Guthi, J. S.; Chin, S. F.; Sherry, A. D.; Boothman, D. A.; Gao, J. M., Multifunctional polymeric micelles as cancer-targeted, MRI-ultrasensitive drug delivery systems. *Nano Letters* **2006,** 6, (11), 2427-2430.
14. Ranger, M.; Jones, M. C.; Yessine, M. A.; Leroux, J. C., From well-defined diblock copolymers prepared by a versatile atom transfer radical polymerization method to supramolecular assemblies. *Journal of Polymer Science Part a-Polymer Chemistry* **2001,** 39, (22), 3861-3874.
15. Colfen, H., Double-hydrophilic block copolymers: Synthesis and application as novel surfactants and crystal growth modifiers. *Macromolecular Rapid Communications* **2001,** 22, (4), 219-252.
16. Riess, G., Micellization of block copolymers. *Progress in Polymer Science* **2003,** 28, (7), 1107-1170.
17. Nakashima, K.; Bahadur, P., Aggregation of water-soluble block copolymers in aqueous solutions: Recent trends. *Advances in Colloid and Interface Science* **2006,** 123, 75-96.
18. Bronich, T. K.; Kabanov, A. V.; Kabanov, V. A.; Yu, K.; Eisenberg, A., Soluble complexes from poly(ethylene oxide)-block-polymethacrylate anions and N-alkylpyridinium cations. *Macromolecules* **1997,** 30, (12), 3519-3525.

19. Wang, Y. P.; Han, P.; Xu, H. P.; Wang, Z. Q.; Zhang, X.; Kabanov, A. V., Photocontrolled Self-Assembly and Disassembly of Block Ionomer Complex Vesicles: A Facile Approach toward Supramolecular Polymer Nanocontainers. *Langmuir* **2010,** 26, (2), 709-715.
20. Gaucher, G.; Dufresne, M. H.; Sant, V. P.; Kang, N.; Maysinger, D.; Leroux, J. C., Block copolymer micelles: preparation, characterization and application in drug delivery. *Journal of Controlled Release* **2005,** 109, (1-3), 169-188.
21. Waiczies, H.; Lepore, S.; Janitzek, N.; Hagen, U.; Seifert, F.; Ittermann, B.; Purfurst, B.; Pezzutto, A.; Paul, F.; Niendorf, T.; Waiczies, S., Perfluorocarbon Particle Size Influences Magnetic Resonance Signal and Immunological Properties of Dendritic Cells. *Plos One* **2011,** 6, (7), 9.
22. Papisov, M. I.; Bogdanov, A.; Schaffer, B.; Nossiff, N.; Shen, T.; Weissleder, R.; Brady, T. J., COLLOIDAL MAGNETIC-RESONANCE CONTRAST AGENTS - EFFECT OF PARTICLE SURFACE ON BIODISTRIBUTION. *Journal of Magnetism and Magnetic Materials* **1993,** 122, (1-3), 383-386.
23. Chen, J. J.; Lanza, G. M.; Wickline, S. A., Quantitative magnetic resonance fluorine imaging: today and tomorrow. *Wiley Interdisciplinary Reviews-Nanomedicine and Nanobiotechnology* **2010,** 2, (4), 431-440.
24. Cabral, H.; Kataoka, K., Multifunctional nanoassemblies of block copolymers for future cancer therapy. *Science and Technology of Advanced Materials* **2010,** 11, (1), 9.
25. Bronich, T. K.; Popov, A. M.; Eisenberg, A.; Kabanov, V. A.; Kabanov, A. V., Effects of block length and structure of surfactant on self-assembly and solution behavior of block ionomer complexes. *Langmuir* **2000,** 16, (2), 481-489.
26. Kabanov, A. V.; Bronich, T. K.; Kabanov, V. A.; Yu, K.; Eisenberg, A., Soluble stoichiometric complexes from poly(N-ethyl-4-vinylpyridinium) cations and poly(ethylene oxide)-block-polymethacrylate anions. *Macromolecules* **1996,** 29, (21), 6797-6802.
27. Li, Y.; Ikeda, S.; Nakashima, K.; Nakamura, H., Nanoaggregate formation of poly(ethylene oxide)-b-polymethacrylate copolymer induced by cationic anesthetics binding. *Colloid and Polymer Science* **2003,** 281, (6), 562-568.

28. Li, Y.; Nakashima, K., Fluorescence studies on the properties of the nanoaggregates of poly(ethylene oxide)-b-polymethacrylate copolymer formed by binding of cationic surfactants to polymethacrylate block. *Langmuir* **2003,** 19, (3), 548-553.
29. Blanazs, A.; Armes, S. P.; Ryan, A. J., Self-Assembled Block Copolymer Aggregates: From Micelles to Vesicles and their Biological Applications. *Macromolecular Rapid Communications* **2009,** 30, (4-5), 267-277.
30. Shuai, X. T.; Ai, H.; Nasongkla, N.; Kim, S.; Gao, J. M., Micellar carriers based on block copolymers of poly(e-caprolactone) and poly(ethylene glycol) for doxorubicin delivery. *Journal of Controlled Release* **2004,** 98, (3), 415-426.
31. Adams, M. L.; Lavasanifar, A.; Kwon, G. S., Amphiphilic block copolymers for drug delivery. *Journal of Pharmaceutical Sciences* **2003,** 92, (7), 1343-1355.
32. Bajpai, A. K.; Shukla, S. K.; Bhanu, S.; Kankane, S., Responsive polymers in controlled drug delivery. *Progress in Polymer Science* **2008,** 33, (11), 1088-1118.
33. Lemal, D. M., Perspective on fluorocarbon chemistry. *Journal of Organic Chemistry* **2004,** 69, (1), 1-11.
34. Matsuda, T.; Annaka, M., Salt effect on complex formation of neutral/polyelectrolyte block copolymers and oppositely charged surfactants. *Langmuir* **2008,** 24, (11), 5707-5713.
35. Jeon, S. I.; Lee, J. H.; Andrade, J. D.; Degennes, P. G., PROTEIN SURFACE INTERACTIONS IN THE PRESENCE OF POLYETHYLENE OXIDE .1. SIMPLIFIED THEORY. *Journal of Colloid and Interface Science* **1991,** 142, (1), 149-158.
36. Lee, J. H.; Lee, H. B.; Andrade, J. D., BLOOD COMPATIBILITY OF POLYETHYLENE OXIDE SURFACES. *Progress in Polymer Science* **1995,** 20, (6), 1043-1079.
37. Pispas, S., Double hydrophilic block copolymers of sodium (2-sulfamate-3-carboxylate) isoprene and ethylene oxide. *Journal of Polymer Science Part a-Polymer Chemistry* **2006,** 44, (1), 606-613.